JOURNAL OF VIROLOGY, Nov. 1994, p. 7320–7328
0022-538X/94/$04.00+0

Vol. 68, No. 11

Epstein-Barr Virus Infection Induces Expression in B Lymphocytes of a Novel Gene Encoding an Evolutionarily Conserved 55-Kilodalton Actin-Bundling Protein

GEORGE MOSIALOS,[1] SHIGEKO YAMASHIRO,[2] ROBERT W. BAUGHMAN,[3] PAUL MATSUDAIRA,[4] LISA VARA,[1] FUMIO MATSUMURA,[2] ELLIOTT KIEFF,[1]* AND MARK BIRKENBACH[1]†

Departments of Medicine and of Microbiology and Molecular Genetics,[1] and Department of Neurobiology,[3] Harvard Medical School, Boston, Massachusetts 02115; Department of Molecular Biology and Biochemistry, Rutgers University, Piscataway, New Jersey 08854[2]; and Whitehead Institute for Biomedical Research and Department of Biology, Massachusetts Institute of Technology, Cambridge, Massachusetts 02142[4]

Received 29 June 1994/Accepted 1 August 1994

A novel human mRNA whose expression is induced over 200-fold in B lymphocytes by latent Epstein-Barr virus (EBV) infection was reverse transcribed, cloned, and sequenced. The mRNA is predicted to encode a protein containing four peptides which precisely match amino acid sequences from a previously identified 55-kDa actin-bundling protein, p55. In vitro translation of the cDNA results in a 55-kDa protein which binds to actin filaments in the presence of purified p55 from HeLa cells. The p55 mRNA is undetectable in non-EBV-infected B- and T-cell lines or in a myelomonocytic cell line (U937). Newly infected primary human B lymphocytes, EBV-transformed B-cell lines, latently infected Burkitt tumor cells expressing EBNA2 and LMP1, a chronic myelogenous leukemia cell line (K562), and an osteosarcoma cell line (TK143) contain high levels of p55 mRNA or protein. In EBV-transformed B cells, p55 localizes to perinuclear cytoplasm and to cell surface processes that resemble filopodia. The p55 mRNA is detected at high levels in spleen and brain tissues, at moderate levels in lung and placenta tissues, and at low levels in skeletal muscle, liver, and tonsil tissues and is undetectable in heart, kidney, pancreas, and bone marrow tissues. Immunohistochemical staining of human brain tissue demonstrates p55 localization to the perinuclear cytoplasm and dendritic processes of many, but not all, types of cortical or cerebellar neurons, to glial cells, and to capillary endothelial cells. In cultured primary rat neurons, p55 is distributed throughout the perinuclear cytoplasm and in subcortical filamentous structures of dendrites and growth cones. p55 is highly evolutionarily conserved since it shows 40% amino acid sequence identity to the *Drosophila singed* gene product and 37% identity to fascin, an echinoderm actin-bundling protein. The evolutionary conservation of p55 and its lack of extensive homology to other actin-binding proteins suggest that p55 has specific microfilament-associated functions in cells in which it is differentially expressed, including neural cells and EBV-transformed B lymphocytes.

Epstein-Barr virus (EBV) can establish a latent infection in primary human B lymphocytes that is characterized by the expression of 10 viral genes and perpetual cell proliferation (16). These infected cells display a pattern of cell gene expression different from that in resting B lymphocytes and similar to that in primary B lymphocytes proliferating in response to stimulation by antigens or mitogens. The differential expression of cellular genes in latently infected B lymphocytes is mediated by one or more viral genes (7, 11, 15, 18, 29–32).

Since EBV-negative Burkitt's lymphoma (BL) cells can be grown in vitro as continuous cell lines, these cells can be used to study the effects of EBV genes on B lymphocytes. BL cells do not express most of the genes whose expression is upregulated by EBV infection of primary B lymphocytes. EBV infection of BL cells normally results in upregulation of these cellular genes. To identify novel cell genes whose expression is upregulated by EBV infection, cDNAs were generated from mRNA of a BL cell line that was infected with EBV in vitro (BL41/B95-8). The specifically upregulated genes were then identified by screening the cDNA library with BL41/B95-8 mRNA-cDNA probes from which the cDNAs complementary to mRNAs expressed in EBV-negative BL41 cells were depleted by subtractive hybridization (6). In this article we describe a novel EBV-induced mRNA that encodes an unusual actin-bundling protein that is differentially expressed in EBV-transformed B lymphocytes and in certain normal tissues including specific neurons of the central nervous system.

* Corresponding author. Mailing address: Infectious Disease Division, Brigham & Women's Hospital, 75 Francis St., Boston, MA 02115. Phone: (617) 732-7048. Fax: (617) 278-6964.

† Present address: Marjorie B. Kovler Viral Oncology Laboratories, University of Chicago, Chicago, IL 60637.

MATERIALS AND METHODS

cDNA cloning and plasmid construction. A cDNA library was prepared from polyadenylated BL41/B95-8 RNA by using the bacteriophage vector lambda gt10. The library was screened by subtractive hybridization (6). cDNA inserts from isolated clones were obtained by *Eco*RI restriction endonuclease digestion and subcloned into pBluescript II SK for further analysis. Clone pBS18.1 contained the 2.7-kb EBI-7 cDNA. The EBI-7 cDNA was also subcloned in either orientation into the *Eco*RI site of M13mp19 for sequencing of GC-rich regions and into the *Eco*RI site of pSG5 (Stratagene) for eukaryotic expression.

Sequencing analysis. The EBI-7 cDNA was sequenced by using the Sequenase kit (United States Biochemical) and

custom-made oligonucleotide primers. GC-rich regions of the cDNA were sequenced by using single-stranded DNA as a template and dITP. The nucleotide sequence of EBI-7 was compared with the sequences present in the National Center for Biotechnology Information databases by using the BLAST algorithm (4). The databases were accessed through the Molecular Biology Computer Research Resource of the Dana-Farber Cancer Institute. The amino acid sequence alignment was performed by using the Clustal program (PCGene; IntelliGenetics, Mountain View, Calif.). The prediction of protein secondary structure was made by using the Garnier algorithm (13).

Cell cultures. BL41 and BJAB are EBV-negative BL cell lines. BL41/B95-8 is an EBV-positive BL cell line that was derived by in vitro infection of the BL41 cell line with the EBV strain B95-8 (10). IB4 is a lymphoblastoid cell line generated by infection of human B lymphocytes with the EBV strain B95-8. AC18 is a lymphoblastoid cell line derived in vitro by infection of primary human B cells with EBV generated by five-cosmid recombination in the P3HR1 cell line (28). TK143 is a human osteosarcoma cell line. K562 is a human chronic myelogenous leukemia cell line. U937 is a histiocytic lymphoma cell line with features characteristic of monocytes. HL60 is a promyelocytic leukemia cell line. MOLT-4 and Jurkat are human T-lymphoblastic leukemia cell lines. SLA is a B-lymphoblastoid cell line generated by EBV transformation of B lymphocytes from a patient with leukocyte adhesion deficiency. These cells fail to express functional LFA-1 on their surface because of a defect in CD18 synthesis and do not form large multicellular aggregates in culture. Primary B lymphocytes were prepared from human peripheral blood mononuclear cells as previously described (25). Five million primary cells were infected with approximately 5×10^6 transforming units of B95-8 virus. Whole-cell lysates were prepared from 2.5×10^5 infected cells at various times postinfection and analyzed by Western blot (immunoblot).

Northern blots. Total RNA or poly(A)$^+$ RNA from various cell lines was size fractionated and transferred to charged nylon membranes (GeneScreen Plus; DuPont, Billerica, Mass.) (6). A Northern (RNA) blot which contained 2 μg each of poly(A)$^+$ RNAs from human heart, brain, placenta, lung, liver, skeletal muscle, kidney, and pancreas tissues was purchased from Clontech. The *Eco*RI fragment of EBI-7 cDNA was labeled by random hexanucleotide priming (Boehringer Mannheim) using [^{32}P]dCTP and was used to detect EBI-7 mRNA. Blots were hybridized overnight at 42°C in 50% formamide–6× SSPE–(1× SSPE is 0.15 M NaCl, 10 mM NaH_2PO_4, and 1 mM EDTA [pH 7.4])–1% sodium dodecyl sulfate (SDS)–1× Denhardt's solution–100 μg of sheared single-stranded herring testis DNA per ml. Filters were washed according to the manufacturer's protocol, with two high-stringency washes at 65 or 70°C in 0.2× SSPE–1% SDS–0.05% sodium pyrophosphate. Washed filters were exposed to autoradiography film (X-Omat AR; Eastman Kodak) for 1 to 3 days at −75°C.

Western blots. BJAB cells (15×10^6) were electroporated with 50 μg of plasmid DNA in 0.4 ml of RPMI 1640 containing 10% fetal calf serum (Sigma) at 200 V and 960 μF. Cells were harvested for Western blot after 12 to 24 h. Whole-cell lysates were generated by boiling the cells in SDS loading buffer for 10 min. Following electrophoresis in 8.5% polyacrylamide gel, proteins were transferred to nitrocellulose membranes. The p55 protein was detected by using either 55K2 or 55K14 monoclonal antibodies (34) diluted 1:500 or 1:1,000 in phosphate-buffered saline (PBS) containing 0.05% Tween 20 and 3% nonfat dry milk. An alkaline phosphatase-conjugated goat anti-mouse antibody (Promega) was used at a 1:5,000 dilution as secondary antibody for the chromogenic detection of protein bands.

Immunofluorescence and immunohistochemical staining. EBV-transformed lymphocytes were dried onto multiwell slides and fixed in absolute methanol at −20°C for 5 min. Primary cultures of rat cerebral cortex (5) were fixed in absolute methanol at −20°C for 5 min. The cells were blocked with PBS containing 20% goat serum for 30 min, incubated at 37°C for 1 h with 55K2 (diluted 1:500), washed five times for 4 min each time with PBS containing 20% goat serum, and incubated with fluorescein isothiocyanate-conjugated or rhodamine-conjugated goat anti-mouse antibody (Jackson ImmunoResearch Laboratories, Inc.). The cells were subsequently washed five times in PBS, mounted, and visualized with a Zeiss Axioskop. Samples of normal human cerebral cortex were obtained postmortem and frozen in dry ice-isopentane. Frozen sections were mounted, air dried, and fixed in a 50:50 mixture of acetone-methanol at −20°C for 20 min. Rehydrated sections were stained with the 55K2 or 55K14 monoclonal antibodies at a 1:1,000 dilution and Texas Red-conjugated goat anti-mouse secondary antibody.

For immunohistochemical analyses, formalin-fixed, paraffin-embedded samples of postmortem or surgically excised human cerebral cortex or cerebellum were deparaffinized, rehydrated, and incubated with a 1:1,000 dilution of a mixture of 55K2 and 55K14. Staining was done with avidin-biotin-complexed horseradish peroxidase by using diaminobenzidine as a chromogen.

Peptide sequencing. The 55-kDa actin-bundling protein was purified from HeLa cells digested with trypsin or cyanogen bromide, and the generated peptides were separated by reversed-phase and sequenced by using Applied Biosystems model 475 and Beckman 2090E gas phase sequenators.

Actin-binding assay. The EBI-7 cDNA was in vitro transcribed by using T3 RNA polymerase (Promega) from 5 to 10 μg of pBS18.1 which had been digested with *Hin*dIII. Five micrograms of purified in vitro-transcribed RNA was translated in vitro by using a rabbit reticulocyte lysate (Promega) in the presence of [^{35}S]methionine and a final volume of 50 μl. Thirty microliters of in vitro translation products was mixed with F-actin (at a final concentration of 12 μM) in a total volume of 60 μl in a buffer containing 20 mM imidazole (pH 7.0) and 100 mM KCl. Increasing amounts (from 0 to 4 μM) of the 55-kDa actin-bundling protein from HeLa cells were added to the actin binding reaction mixture. The samples were incubated for 1 h at room temperature and centrifuged in a Beckman Airfuge at 26 lb/in^2 for 30 min. Both supernatants and pellets were analyzed by SDS-polyacrylamide gel electrophoresis and fluorography.

Nucleotide sequence accession number. The DNA sequence reported in this article has been deposited in GenBank under accession number HSU09873.

RESULTS

EBI-7 encodes a human 55-kDa actin-bundling protein. Subtractive hybridization coupled with differential screening of a cDNA library from an EBV-infected BL cell line (6) identified a cDNA clone for an EBV-induced mRNA, EBI-7. The nucleotide and predicted amino acid sequences of EBI-7 are shown in Fig. 1. Comparison of the predicted amino acid sequence with the proteins in the National Center for Biotechnology Information databases indicated that the EBI-7-encoded protein has 40% sequence identity with the protein product of the *Drosophila* developmental gene *singed* (22) and 36.5% identity with the echinoderm actin-bundling protein

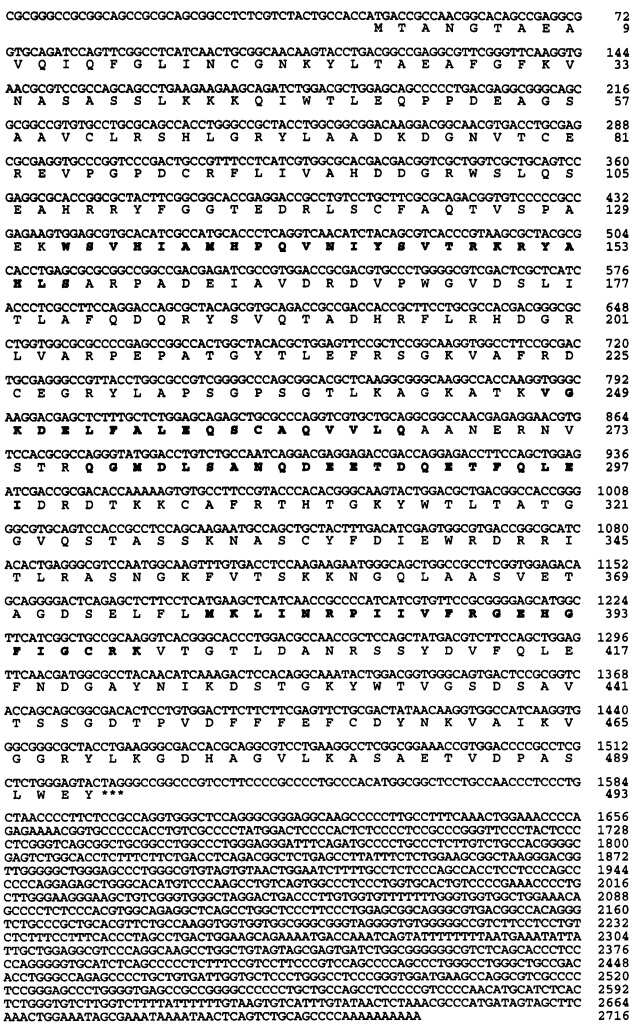

FIG. 1. Nucleotide and deduced amino acid sequence of clone EBI-7. Boldfaced sequences correspond to peptide sequences obtained from purified p55 protein from HeLa cells.

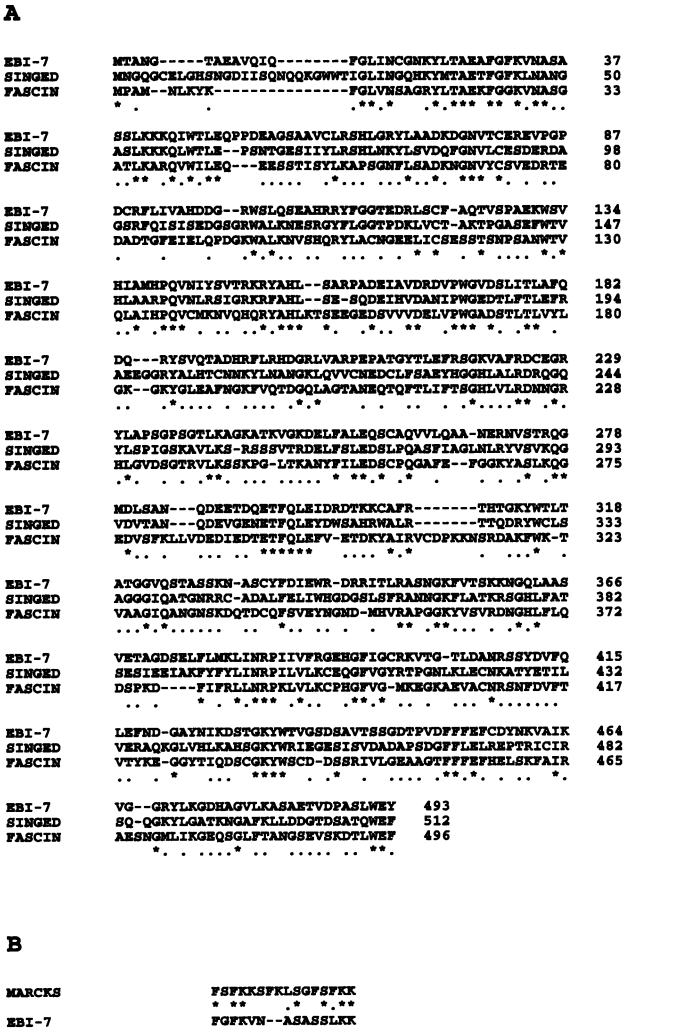

FIG. 2. (A) Amino acid sequence alignment of the predicted human EBI-7, *Drosophila singed* (22), and sea urchin *fascin* (8) gene products. The alignment was performed with the Clustal program (PCGene; IntelliGenetics). Identical (asterisks) and homologous (dots) amino acid residues are indicated. (B) Amino acid sequence alignment between a putative actin-binding motif of p55 (amino acids 29 to 42) and the actin-binding site of MARCKS.

fascin (8). Figure 2A shows an amino acid sequence alignment of EBI-7 with the *Drosophila singed* product and sea urchin fascin. Amino acid homology extends through the entire sequence of each of these proteins. Comparison of the nucleotide sequence of EBI-7 with the nucleotide sequences in the National Center for Biotechnology Information databases also identified 99% identity of the 3′ untranslated sequence to three sequence tags (EST01023, EST00182, and EST01645) from human brain cDNA libraries (1, 2). EBI-7 also has a 14-amino-acid segment located near the amino-terminal end (amino acids 29 to 42) which shows significant sequence similarity to the actin-binding site of MARCKS (Fig. 2B) (3). This region is believed to form an α helix in MARCKS (3) and is predicted to attain an α-helical conformation in EBI-7 by the Garnier algorithm (13). No other significant homology between EBI-7 and actin-binding proteins was identified.

The similarity of EBI-7 to fascin prompted us to examine the relationship of EBI-7 with a human 55-kDa actin-bundling protein, p55, that had been previously purified from HeLa cells (33). The sequences of peptides derived from partial proteolysis of affinity-purified p55 from HeLa cells were as follows (amino acids predicted with low probabilities are boldfaced; X, unidentified residue): WSVHIAMHPQVNIYXVTXKXXAH LS (40 kDa), VGKDELFALEQSXAQVVLQ (30 kDa), QG MDLSANQDEETDQETFQLEI (25 kDa), and MKLINRPI IVFRGEHGFIGXRK (size not determined) (the last peptide was obtained with cyanogen bromide; the other peptides were obtained with trypsin). The peptides showed precise identity with sequences from the predicted translation product of the EBI-7 gene and a high degree of homology with peptide sequences from singed and fascin (Fig. 1 and 2A). The sizes of the tryptic peptides from p55 are also consistent with that of the predicted EBI-7 translation product (Fig. 1). Two monoclonal antibodies raised against p55 reacted with the EBI-7-encoded protein expressed in the BJAB BL cell line (Fig. 3). The EBV-transformed cell line AC18, the EBV-positive BL cell line BL41/B95-8, and BJAB cells transfected with an EBI-7 expression construct contain a 55-kDa protein that reacts with

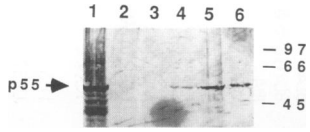

FIG. 3. Western blot analysis of p55 expression in various cell lines. Whole-cell lysates were prepared by boiling the cells in SDS loading buffer; they were analyzed on an SDS–8.5% polyacrylamide gel, and they were transferred onto nitrocellulose. Immunoblotting was performed with the 55K2 monoclonal antibody as the primary antibody and alkaline phosphatase-conjugated goat anti-mouse as secondary antibody. Lane 1, whole-cell extract from 7×10^5 BJAB cells transfected with pSG5 containing the EBI-7 cDNA; lane 2, whole-cell extract from 7×10^5 BJAB cells transfected with pSG5; lane 3, whole-cell extract from 4×10^5 BL41 cells; lane 4, whole-cell extract from 2×10^5 BL41/B95-8 cells; lane 5, whole-cell extract from 2×10^5 AC18 cells; lane 6, purified p55 protein from HeLa cells. The position of p55 protein is indicated.

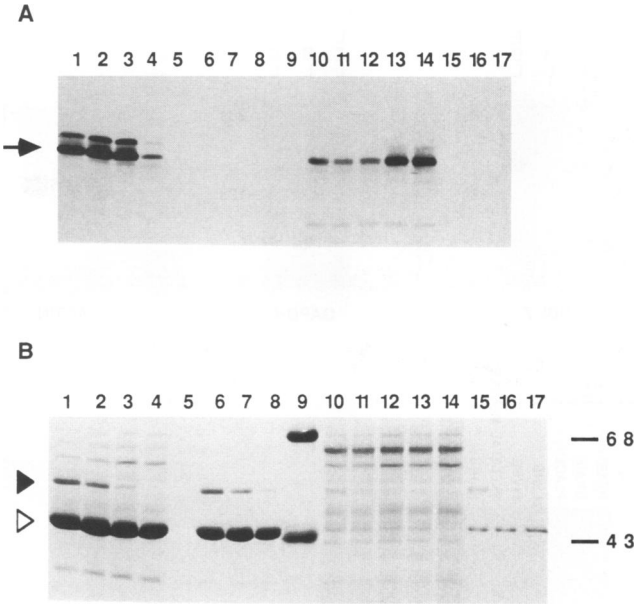

FIG. 4. Actin-binding properties of p55 protein synthesized by in vitro translation of EBI-7 RNA. The actin-binding ability of radiolabeled in vitro-translated p55 protein was tested in the absence or presence of unlabeled purified p55, by mixing 30 μl of the in vitro translation reaction mix with F-actin. Following incubation at room temperature for 1 h the reaction mixture was centrifuged and the pellets (lanes 1 through 8) and supernatants (lanes 10 through 17) were analyzed by SDS-polyacrylamide gel electrophoresis followed by Coomassie blue staining (B) and fluorography (A). Lanes 1 and 10, 0.22 mg of unlabeled p55 per ml–0.5 mg of actin per ml–30 μl of in vitro translation products; lanes 2 and 11, 0.11 mg of unlabeled p55 per ml–0.5 mg of actin per ml–30 μl of in vitro translation products; lanes 3 and 12, 0.06 mg of unlabeled p55 per ml–0.5 mg of actin per ml–30 μl of in vitro translation products; lanes 4 and 13, 0.5 mg of actin per ml–30 μl of in vitro translation products; lanes 5 and 14, 30 μl of in vitro translation products; lanes 6 and 15, 0.22 mg of unlabeled p55 per ml–0.5 mg of actin per ml; lanes 7 and 16, 0.11 mg of unlabeled p55 per ml–0.5 mg of actin per ml; lanes 8 and 17, 0.06 mg of unlabeled p55 per ml–0.5 mg of actin per ml; lanes 9, molecular weight markers. The sizes of the molecular weight markers are shown in kilodaltons on the right in panel B. Arrow and closed arrowhead, position of p55; open arrowhead position of actin.

the 55K2 monoclonal antibody (Fig. 3). No 55-kDa protein was detected in the EBV-negative cell line BL41 or in BJAB cells transfected with the expression vector pSG5 alone (Fig. 3). The same pattern was observed when another anti-p55 monoclonal antibody (55K14) was used as the primary antibody in the immunoblotting experiment (data not shown). Thus, the size of the EBI-7-encoded protein, its reactivity with two different p55-specific monoclonal antibodies, and the identity of its predicted amino acid sequence with the sequences of four different peptides from p55 indicate that the EBI-7 gene encodes p55.

Previous studies using affinity-purified protein demonstrated that p55 can bundle actin filaments in vitro (33). The ability of the EBI-7-encoding protein to bind actin filaments was therefore assayed directly by using in vitro-translated protein. In vitro transcription coupled with in vitro translation of EBI-7 produced a 55-kDa protein as the major product (Fig. 4A, lane 14) which comigrated with purified p55 from HeLa cells, as determined by aligning the autoradiogram shown in Fig. 4A with the Coomassie blue-stained gel shown in Fig. 4B. Incubation of the in vitro-translated p55 with F-actin resulted in association of a small proportion of p55 with actin filaments (Fig. 4A; compare lanes 4 and 13). The concentration of in vitro-translated p55 in the in vitro translation reaction is estimated to be significantly below the micromolar range, as determined by the inability to detect 55-kDa protein bands in Coomassie blue-stained in vitro translation products (Fig. 4B, lane 14). Since the dissociation constant of the interaction of p55 with actin has been estimated to be in the micromolar range and p55 binds to actin in a cooperative fashion, the addition of purified p55 to the actin-binding reaction should enhance the binding of in vitro-translated p55. The actin-binding ability of a fixed amount of radiolabeled in vitro-translated p55 protein was therefore assayed in the presence of increasing amounts of purified p55 from HeLa cells. Addition of 1 μM p55 from HeLa cells significantly increased the amount of actin-associated in vitro-translated p55 protein (Fig. 4A; compare lanes 3 and 4). When the concentration of purified p55 was increased to 2 μM, the amount of in vitro-translated p55 associated with actin filaments was increased by 30% compared with the amount of p55 that bound actin in the presence of 1 μM purified p55 (Fig. 4A; compare lanes 2 and 3) (radioactivity was quantified by Phosphorimager analysis). Finally, 4 μM purified p55 competed with in vitro-translated p55 for actin binding, and the amount of actin-associated in vitro-translated p55 was reduced by 38% compared with the amount that bound actin at 1 μM purified p55 (Fig. 4A; compare lanes 1 and 3). Competition is observed because actin-binding of p55 is nearly saturated at 4 μM under the conditions of this experiment (33). Thus, EBI-7 encodes a protein which shares the physiologic properties of the p55 actin-bundling protein.

Cell line- and tissue-specific EBI-7 expression. EBI-7 mRNA expression was evaluated in EBV-positive and -negative B-cell lines and in continuous cell lines from other tissues. A 3.0-kb polyadenylated RNA was found in the EBV-transformed lymphoblastoid cell line IB4 and in the EBV-converted BL cell line BL41/B95-8, but it was not detectable in EBV-negative BL41 cells (Fig. 5A). Each lane had similar amounts of β actin and glyceraldehyde phosphate dehydrogenase mRNA except for the BL41 lane which was overloaded with respect to both control RNAs. Analysis of cytoplasmic RNAs from several additional human lymphoid cell lines failed to detect EBI-7 RNA in any EBV-negative BL cell line (Louckes, BL30, or BL41) or T-cell line (Jurkat or MOLT-4) (Fig. 5B). However, all EBV-transformed lymphoblastoid cell lines (IB4,

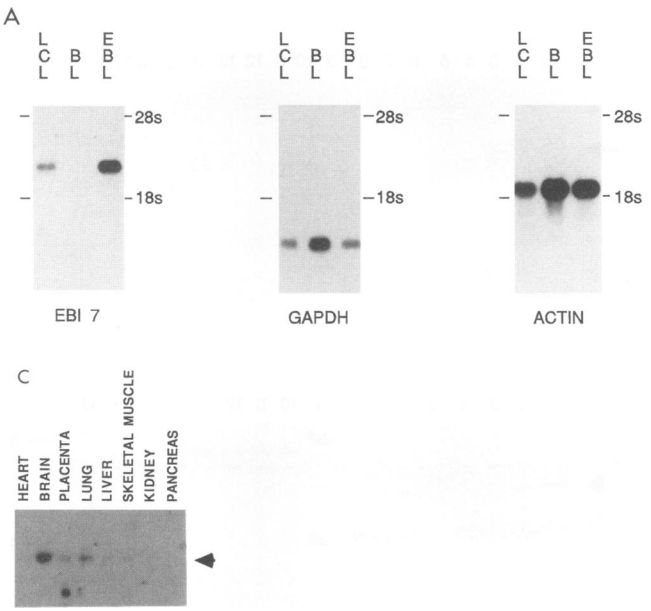

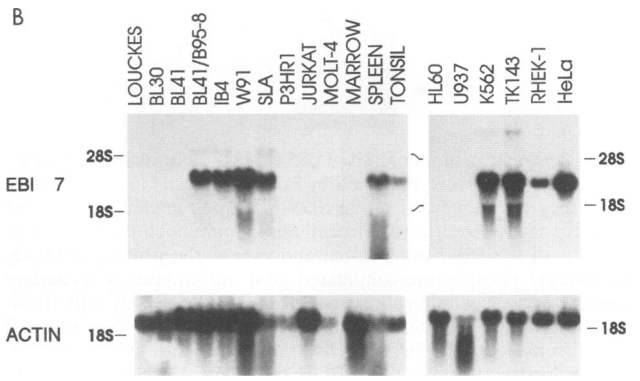

FIG. 5. EBI-7 RNA expression in human cell lines and tissues. (A) Parallel blots containing polyadenylated RNA from the EBV-negative BL cell line BL41 (12 μg of RNA), its EBV-converted derivative BL41/B95-8 (EBL) (4 μg of RNA), and the EBV-transformed lymphoblastoid cell line (LCL) IB4 (4 μg of RNA) were hybridized with the probes indicated at the bottom. The amounts of RNA loaded in each lane were assessed with control probes specific for β-actin and glyceraldehyde phosphate dehydrogenase (GAPDH). (B) The EBI-7 probe was hybridized to blots containing RNA (12 μg per lane) from human lymphoid cell lines and tissues indicated at the top. Louckes, BL30, and BL41, EBV-negative BL cell lines; BL41/B95-8, an EBV-converted BL line; IB4, W91, and SLA, EBV-transformed lymphoblastoid cell lines; P3HR1, a BL cell line infected with the nontransforming EBV strain P3HR1; Jurkat and MOLT-4, T-lymphocyte cell lines; Marrow, human postmortem rib marrow; Spleen and Tonsil, surgically excised human spleen and tonsil. The EBI-7 probe was also hybridized to 12 μg of cytoplasmic RNA (HL60, U937, and K562), total cellular RNA (TK143), or 2 μg of polyadenylated RNA (RHEK-1 and HeLa). (C) Northern blot analysis of tissue distribution of EBI-7. A multitissue Northern blot, containing 2 μg of polyadenylated RNA from each one of eight human tissues, was obtained from Clontech. The blot was hybridized to a probe made from the *Eco*RI fragment of EBI-7 cDNA. The sources of the RNAs are indicated. Arrow, position of the EBI-7 mRNA.

W91, and SLA) expressed abundant EBI-7 mRNA (Fig. 5B). EBI-7 mRNA is also not expressed by the P3HR1 cell line, which is a BL cell line infected with an EBV deletion mutant that fails to express EBV nuclear proteins EBNA-LP and EBNA2 and the latent-infection-associated integral membrane protein LMP1 (Fig. 5B). EBI-7 RNA is also expressed abundantly in some human non-lymphoid-transformed cell lines of epithelial (HeLa and RHEK-1), mesenchymal (TK143), and myeloid (K562) origins, but it is not detectable in the HL60 or U937 myeloid lines (Fig. 5B).

The expression of EBI-7 mRNA in normal human tissues was also examined by hybridizing labeled EBI-7 cDNA to a tissue RNA blot (Fig. 5C). The EBI-7 mRNA was highly expressed in adult-human brain tissue (Fig. 5C). Lung tissue contained moderate levels of EBI-7 mRNA, while placenta, liver, and skeletal muscle tissues contained smaller amounts. EBI-7 mRNA was not detected in heart, kidney, or pancreas tissue (Fig. 5C).

To investigate whether infection of primary B lymphocytes with EBV leads to induction of p55, human peripheral blood mononuclear cells enriched for B cells were infected with the B95-8 strain of EBV at a multiplicity of infection of approximately 1. p55 was assayed by Western blot in whole-cell lysates from equal numbers of cells at different times postinfection (Fig. 6). As expected, p55 was not detectable in uninfected cells (Fig. 6, lane 5). At 2 h, 1 day, or 2 days postinfection, neither EBNAs nor p55 was detectable (Fig. 6, lanes 4, 3, and 2, respectively). However, at 8 days postinfection p55, EBNA1, and EBNA2 were all expressed at significant levels that were lower than the levels of established lymphoblastoid cell lines (Fig. 6, lane 1). This and two additional independent primary B-lymphocyte infections (data not shown) indicate that p55 is induced in primary B lymphocytes during the process of establishing growth transformation.

Localization of p55 in EBV-transformed B lymphocytes, neurons, and brain tissue. Indirect immunofluorescence staining of EBV-transformed B lymphocytes demonstrated p55 distribution in a perinuclear cytoplasmic pattern and localization to cell surface processes that resemble filopodia (Fig. 7a and b). This staining pattern is similar to previous p55 localization observed in stress fibers and microspikes of gerbil fibroma cells (34).

Because of the finding of a high level of EBI-7 mRNA in human brain tissue, the intracellular localization of p55 was evaluated in primary brain cell cultures. Cultures of rat cerebral cortex were used since previous studies with the anti-p55 monoclonal antibodies demonstrated broad mammalian species reactivity. p55 localized in the cytoplasm of the neuronal cell body and to subcortical filaments in axons and dendrites. The staining of axonal and dendritic filaments was periodically accentuated (Fig. 7c and d). Neuronal growth cones stained intensely, suggesting a role for p55 in growth cone function (Fig. 7c and d). Weaker staining was observed along stress fibers of glial cells (Fig. 7e). Control slides of rat neuronal cultures stained only with the goat anti-mouse secondary antibody were negative (Fig. 7f).

Immunostaining of normal human brain tissue demonstrated cell-type-specific expression of p55 protein in both neurons and glial cells. Immunoperoxidase staining of formalin-fixed cerebellum tissue demonstrated p55 in perikarya and processes of stellate cell neurons of the outer cerebellar cortex (Fig. 8A). Neuronal staining was cell type specific, however, as Purkinje and granular cell bodies and their respective processes failed to exhibit p55 reactivity (Fig. 8B). The majority of white matter glial cells stained intensely, though a subpopulation of glial cells failed to stain (Fig. 8C). Many of the p55-positive glial cells exhibited morphological features sug-

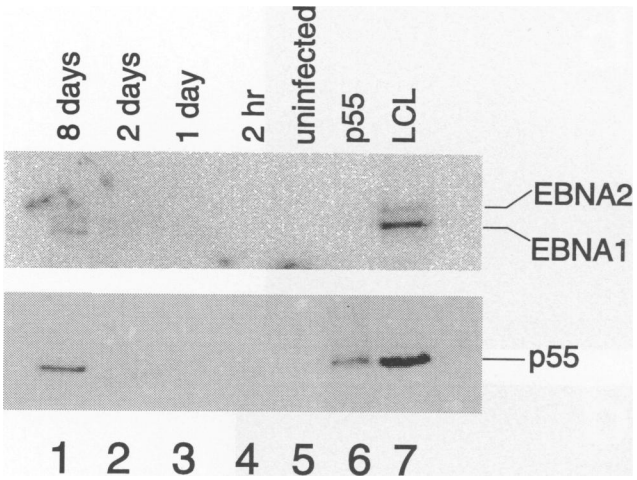

FIG. 6. Induction of p55 by infection of primary B lymphocytes with EBV. Human peripheral blood mononuclear cells enriched for B cells were infected with EBV strain B95-8 as described in Materials and Methods. Whole-cell lysates from 2.5×10^5 cells of an established lymphoblastoid cell line (lane 7), uninfected primary cells (lane 5), or EBV-infected primary cells at the indicated times postinfection were analyzed by Western blot. A sample of purified p55 from HeLa cells was also run in parallel as a control (lane 5). p55 was detected with the 55K2 monoclonal antibody as the primary antibody and alkaline phosphatase-conjugated goat anti-mouse as a secondary antibody (lower panel). The latent antigens EBNA1 and EBNA2 were detected with a 1/50 dilution of human serum (upper panel) as previously described (25).

gestive of oligodendrocytes, with small round-to-oval nuclei and tapering, bipolar processes. In addition, diffuse fibrillar staining of the white matter was observed (Fig. 8C). The detection of p55 in both neuronal processes and glial cells likely reflects p55 expression in both axons and oligodendrocyte-derived myelin sheaths. A similar expression pattern was observed in temporal lobe cortex, with intense staining of both white matter fiber tracts and scattered glial cells (data not shown). Staining of granule cells of the dentate gyrus was weak or undetectable (Fig. 8D). In both cerebral and cerebellar tissue sections, positive staining was also detected in capillary endothelial cells (Fig. 8A and C). Immunofluorescence staining of frozen sections of postmortem parietal lobe cortex detected p55 in neuronal cell bodies in a predominantly perinuclear distribution, with weaker staining of dendritic processes (data not shown). This staining was clearly distinguishable from the autofluorescence of pigment granules in some cell bodies.

DISCUSSION

These findings indicate that a novel cellular gene, whose expression is markedly upregulated in B lymphocytes by EBV infection, encodes the previously identified actin-bundling protein, p55. The predicted sequence of p55 displays significant colinear homology to sea urchin fascin (36.5% amino acid identity) and the *Drosophila singed* gene product (40% amino acid identity). This homology is particularly remarkable, given the lack of significant stretches of colinear homology to other mammalian actin-binding proteins. The degree of amino acid identity among proteins derived from these evolutionarily divergent species suggests that p55 and its homologs may have fundamental and highly conserved roles in microfilament structure or in microfilament-associated functions.

The level of p55 expression varies widely among different tissues and cell types, suggesting that its functions may relate to unique and differentiation-associated features of some specialized cell types. p55 RNA or protein is expressed at high levels in spleen and brain tissues, at moderate levels in lung and placenta tissues, and at significantly lower levels in most other tissues. In brain tissue, high-level expression is characteristic of specific cell types and locations. Wide differences in the level of p55 expression are also evident among cell lines. Expression is high in K562 (a myeloid leukemia cell line), in HeLa and RHEK-1 (epithelial cell lines), and in TK143 (a mesenchymal cell line). Expression in some of these cell lines is probably related to their transformed or abnormally differentiated state since p55 is not normally expressed in bone marrow and is not found in other hematopoietic cell lines such as HL60 or U937. Significantly, among a panel of lymphocytic cell lines, p55 was expressed only in EBV-transformed B lymphocytes or in Burkitt tumor cell lines that express the full repertoire of EBNAs and LMPs and was undetectable in non-EBV-infected B- or T-cell lines that we have examined. It should be noted that the induction of p55 in EBV-transformed B cells is not a secondary effect of cell clumping, since p55 is induced in the EBV-positive B-cell line SLA, which is defective in cell adhesion and does not form cell aggregates.

The intracellular localization of p55 was investigated by indirect immunofluorescence or immunohistochemical staining. In EBV-transformed B lymphocytes, p55 displays a perinuclear cytoplasmic distribution and localizes to filopodium-like cell surface processes. In human brain tissue, p55 localizes to perinuclear cytoplasmic structures and to dendrites of some types of cortical and cerebellar neurons. In neuronal cell cultures, p55 localizes to the cytoplasmic area of the neuronal cell body, to clearly defined filamentous structures along dendrites, and at growth cones. The subcellular distribution of p55 in neurons in vitro and in brain tissue is compatible with a role for this actin-cross-linking protein in neural vesicular transport. p55 could play a role in the organization of microfilaments along the axon or in the interactions of cytoskeletal elements that underlie vesicle fusion and neurotransmitter release.

The tissue distribution and intracellular localization of p55 overlaps significantly with that of MARCKS and GAP-43. MARCKS is an actin-cross-linking protein that is expressed at high levels in brain and spleen tissues (27) and is highly induced in B lymphocytes by EBV infection (6). The intracellular localization of MARCKS has been studied most intensively in macrophages, where it colocalizes with vinculin and talin in the substratum contact points of filopodia and pseudopodia (26). GAP-43 is a neuron-specific protein that localizes to substrate contact points in filopodium-like structures in growth cones of cultured neurons (20). GAP-43 is also capable of inducing filopodium-like cytoplasmic projections in COS cells following gene transfer (35). In EBV-transformed B lymphocytes, p55 staining was prominent in cell surface processes that seemed to be able to extend and retract since their length varied significantly. In neurons, p55 is associated with axonal membranes and growth cones. Since elongation and retraction of these organelles requires rapid reorganization of microfilaments, p55 could be an important factor in this process. In contrast to MARCKS and GAP-43, p55 is associated not only with filopodia and growth cones but also with perinuclear structures in neurons and EBV-transformed lymphocytes. Collectively, these data suggest that p55, GAP-43, and MARCKS may be coordinately regulated to serve com-

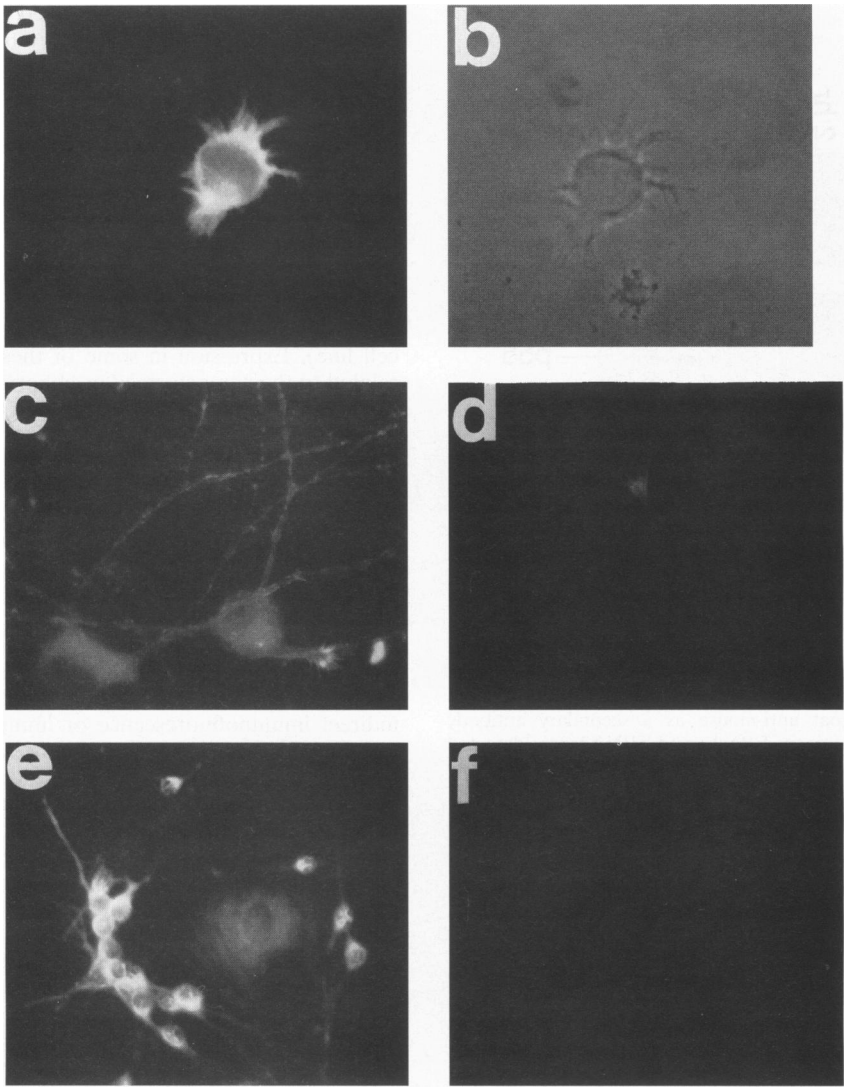

FIG. 7. Immunofluorescence staining of various cultured cells with anti-p55 monoclonal antibodies. Immunofluorescence (a) and phase contrast (b) image of AC18 cells incubated with 55K2 antibody and visualized with fluorescein isothiocyanate-conjugated goat anti-mouse secondary antibody. Strong staining is observed in the perinuclear region and in cell surface processes. (c to e) Immunofluorescence staining of neurons in cultures of rat cerebral cortex with 55K2 and rhodamine-conjugated goat anti-mouse secondary antibody; (f) control with rhodamine-conjugated goat anti-mouse secondary antibody alone. Staining along neurites and especially at growth cones is apparent (c and d). In addition, weaker staining of stress fibers in glial cells is evident (e).

plementary functions in the regulation of the actin cytoskeleton-plasma membrane interactions.

p55 contains a 14-amino-acid sequence that resembles the actin-binding site of MARCKS and the related MacMARCKS/SF52 proteins (3). In all three proteins this domain is predicted to assume an amphipathic α-helical secondary structure, with basic residues toward one side of the helix. In MARCKS, four lysines are important in actin binding and in calcium-calmodulin binding. p55 has two lysines on the same face of the predicted α helix. Another important feature of this domain in MARCKS is the presence of three serines which can be phosphorylated by protein kinase C. Phosphorylation can regulate the association of MARCKS with actin. p55 has one serine (Ser-39) in a consensus protein kinase C recognition site. The predicted hydrophobic side of the putative actin-binding site of p55 consists of phenylalanine, leucine, and valine instead of the three phenylalanines in MARCKS. Since the actin-cross-linking activity of MARCKS is inhibited by calcium-calmodulin or by protein kinase C phosphorylation within the actin-binding site, a similar mechanism may regulate the activity of p55. GAP-43 has a more distantly related basic and serine residue domain which interacts with calmodulin. Another actin-binding protein, villin, contains two lysines important for actin binding that are also predicted to lie on the same face of an α-helical segment (12).

The significant colinear homology of p55 to sea urchin fascin and *Drosophila singed* proteins provides some insight into the role of these proteins in cell biology. Fascin cross-links actin filaments in microvilli that are present in sea urchin eggs and organizes actin filaments into bundles in the filopodia of phagocytic coelomocytes from echinoderms (9). Mutations in *singed* affect primarily the hairs and bristles of adult flies and

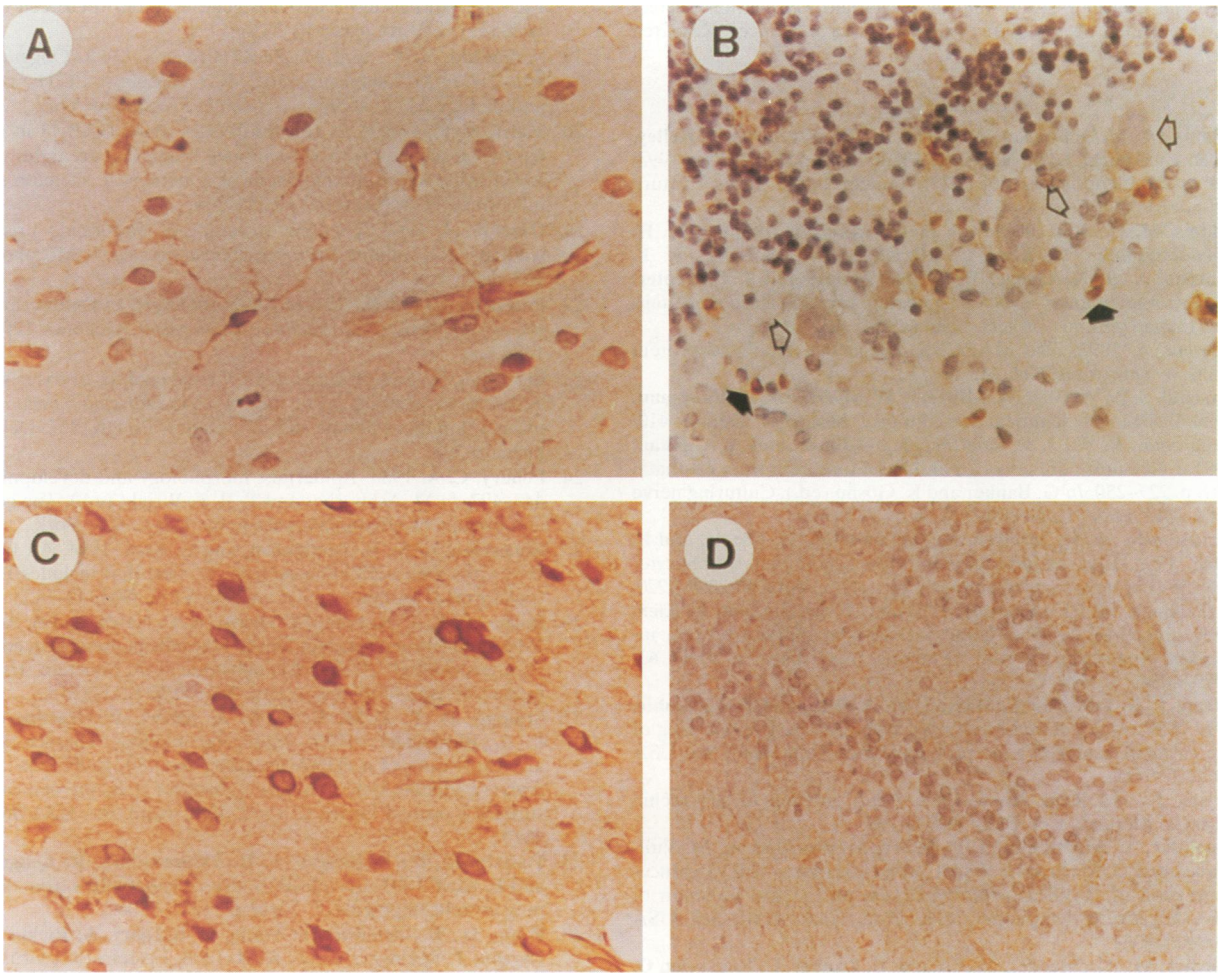

FIG. 8. Immunohistochemical detection of p55 in surgically excised, formalin-fixed human cerebellum. p55 is detected in stellate cell bodies and dendritic processes of outer cerebellar cortex (A). Note also staining of endothelial cells of small blood vessels. p55 expression in cerebellar Purkinje cells (open arrows) and granular cells is weak or undetectable (B). Scattered glial cells of the granular and molecular layers stain intensely (closed arrows). Cerebellar white matter shows intense perinuclear staining of most but not all glial cells and diffuse fibrillar background staining of white matter nerve processes (C). p55 expression in neurons of the dentate gyrus is weak or undetectable (D).

the ovaries of female flies (23, 24). Both large bristles (macrochaetae) and small bristles (microchaetae) are affected, and in general, they are shorter and twisted in *sn* flies compared with wild-type flies. Macrochaetae are composed of four cell types in *Drosophila melanogaster*: the trichogen, which forms the shaft of the bristle, the tormogen, which generates the socket, a sensory cell, and a neurilemma cell (24). The trichogen contains microfilament bundles arranged along the long axis of the bristle shaft around a central core of similarly oriented microtubules (21). In *sn* mutants the number of microfilaments is reduced, thus leading to the formation of a shorter and curved shaft. The homologies between the *singed* product and actin-bundling proteins, p55 (as noted here) and fascin (as noted in another study [8]), provide inferential evidence that the *singed* product is itself an actin-bundling protein. This would explain the phenotype of the *singed* mutations in that a mutant actin-bundling protein might be expected to inhibit bundle assembly and lead to abnormal bristles.

sn mutant flies in most cases also have ovarian defects. Eggs are fewer and less mature. Oocyte maturation in *D. melanogaster* depends on the continuous flow of nutrients from nurse cells into the developing oocyte through interconnecting bridges that are formed by incomplete cytokinesis (reviewed in references 17 and 19). Disruption of actin filaments with cytochalasin prevents the flow of nutrients from nurse cells into the oocyte, thus preventing maturation (14). p55 may be an organizing center for actin microfilaments, which in turn provide structure and a contractile force for the transport of cytoplasmic components into the oocyte in the late stages of maturation. p55 may have an analogous role in human lymphocyte and neural cell biology.

ACKNOWLEDGMENTS

We are grateful to Erle Robertson for help with primary B-cell infection with EBV. We thank Anthony Montag for help with immunohistochemical staining.

This work was supported by grants CA47006 from the National Cancer Institute (to E.K.), CA42742 from the National Cancer Institute (to F.M.), CD442 from the American Cancer Society (to F.M.), and CA44704 from the National Institute of Health (to P.M.). M.B. was supported by a Physician Scientist Award (grant CA01341) from

the National Cancer Institute and by the Gould Foundation Faculty Scholarship Fund of the University of Chicago Cancer Research Center.

REFERENCES

1. **Adams, M., M. Dubnick, A. R. Kerlavage, R. Moreno, J. M. Kelley, T. R. Utterback, J. W. Nagle, C. Fields, and J. C. Venter.** 1992. Sequence identification of 2,375 human brain genes. Nature (London) **355:**632–634.
2. **Adams, M. D., J. M. Kelley, J. D. Gocayne, M. Dubnick, M. H. Polymeropoulos, H. Xiao, C. Merril, A. Wu, B. Olde, R. F. Moreno, A. R. Kerlavage, W. R. McCombie, and J. C. Venter.** 1991. Complementary DNA sequencing: expressed sequence tags and human genome project. Science **252:**1651–1656.
3. **Aderem, A.** 1992. The MARCKS brothers: a family of protein kinase C substrates. Cell **71:**713–716.
4. **Altschul, S. F., W. Gish, W. Miller, E. W. Myers, and D. J. Lipman.** 1990. Basic local alignment search tool. J. Mol. Biol. **215:**403–410.
5. **Baughman, R. W., J. E. Huettner, K. A. Jones, and A. A. Khan.** 1991. Cell culture of neocortex and basal forebrain from postnatal rats, p. 227–250. *In* G. Banker and K. Goslin (ed.), Culturing nerve cells. MIT Press, Cambridge, Mass.
6. **Birkenbach, M., K. Josefsen, R. Yalamanchili, G. Lenoir, and E. Kieff.** 1993. Epstein-Barr virus-induced genes: first lymphocyte-specific G protein-coupled peptide receptors. J. Virol. **67:**2209–2220.
7. **Birkenbach, M., D. Liebowitz, F. Wang, J. Sample, and E. Kieff.** 1989. Epstein-Barr virus latent infection membrane protein increases vimentin expression in human B-cell lines. J. Virol. **63:** 4079–4084.
8. **Bryan, J., R. Edwards, P. Matsudaira, J. Otto, and J. Wulfkuhle.** 1993. Fascin, an echinoid actin-bundling protein, is a homolog of the *Drosophila* singed gene product. Proc. Natl. Acad. Sci. USA **90:**9115–9119.
9. **Bryan, J., and R. E. Kane.** 1982. Actin gelation in sea urchin extracts. Methods Cell Biol. **25:**176–198.
10. **Calendar, A., M. Billaud, J. P. Aubry, M. Banchereau, M. Vuillaume, and G. M. Lenoir.** 1987. Epstein-Barr virus (EBV) induces expression of B-cell activation markers on in vitro infection of EBV-negative B-lymphoma cells. Proc. Natl. Acad. Sci. USA **84:**8060–8064.
11. **Cordier, M., A. Calender, M. Billaud, U. Zimber, G. Rousselet, O. Pavlish, J. Banchereau, T. Tursz, G. Bornkamm, and G. M. Lenoir.** 1990. Stable transfection of Epstein-Barr virus (EBV) nuclear antigen 2 in lymphoma cells containing the EBV P3HR1 genome induces expression of B-cell activation molecules CD21 and CD23. J. Virol. **64:**1002–1013.
12. **Friedrich, E., K. Vancompernolle, C. Huet, M. Goethals, J. Finidori, J. Vandekerckhove, and D. Louvard.** 1992. An actin-binding site containing a conserved motif of charged amino acid residues is essential for the morphogenic effect of villin. Cell **70:** 81–92.
13. **Garnier, J., D. J. Osguthorpe, and B. Robson.** 1978. Analysis of the accuracy and implications of simple methods for predicting the secondary structure of globular proteins. J. Mol. Biol. **120:**97–120.
14. **Gutzeit, H. O.** 1986. The role of microfilaments in cytoplasmic streaming in Drosophila follicles. J. Cell Sci. **80:**159–169.
15. **Henderson, S., M. Rowe, C. Gregory, D. Croom-Carter, F. Wang, R. Longnecker, E. Kieff, and A. Rickinson.** 1991. Induction of bcl-2 expression by Epstein-Barr virus latent membrane protein 1 protects infected B cells from programmed cell death. Cell **65:** 1107–1115.
16. **Kieff, E., and D. Liebowitz.** 1990. Epstein-Barr virus and its replication, p. 1889–1920. *In* B. N. Fields and D. M. Knipe (ed.), Virology, 2nd ed. Raven Press, New York.
17. **King, R. C.** 1970. Ovarian development in Drosophila melanogaster. Academic Press, New York.
18. **Knutson, J. C.** 1990. The level of c-*fgr* RNA is increased by EBNA-2, an Epstein-Barr virus gene required for B-cell immortalization. J. Virol. **64:**2530–2536.
19. **Mahowald, A. P., and M. P. Kambysellis.** 1980. Oogenesis, p. 141–224. *In* M. Ashburner and T. R. F. Wright (ed.), The genetics and biology of Drosophila. Academic Press, New York.
20. **Meiri, K. F., and P. R. Gordon-Weeks.** 1990. GAP-43 in growth cones is associated with areas of membrane that are tightly bound to substrate and is a component of a membrane skeleton subcellular fraction. J. Neurosci. **10:**256–266.
21. **Overton, J.** 1967. The fine structure of developing bristles in wildtype and mutant *Drosophila melanogaster*. J. Morphol. **122:** 367–380.
22. **Paterson, J., and K. O'Hare.** 1991. Structure and transcription of the *singed* locus of *Drosophila melanogaster*. Genetics **129:**1073–1084.
23. **Perrimon, N., and M. Gans.** 1983. Clonal analysis of tissue specific and recessive female-sterile mutations in *Drosophila melanogaster* using a dominant female sterile mutation Fs(1)K1237. Dev. Biol. **100:**365–373.
24. **Poodry, C. A.** 1980. Epidermis: morphology and development, p. 443–497. *In* M. Ashburner and T. R. F. Wright (ed.), The genetics and biology of Drosophila. Academic Press, New York.
25. **Robertson, E. S., B. Tomkinson, and E. Kieff.** 1994. An Epstein-Barr virus with a 58-kilobase-pair deletion that includes BARF0 transforms B lymphocytes in vitro. J. Virol. **68:**1449–1458.
26. **Rosen, A., K. F. Keenan, M. Thelen, A. C. Nairn, and A. Aderem.** 1990. Activation of protein kinase C results in the displacement of its myristoylated, alanine-rich substrate from punctate structures in macrophage filopodia. J. Exp. Med. **172:**1211–1215.
27. **Stumpo, D. J., J. M. Graff, K. A. Albert, P. Greengard, and P. J. Blackshear.** 1989. Molecular cloning, characterization, and expression of a cDNA encoding the "80- to 87-kDa" myristoylated alanine-rich C kinase substrate: a major cellular substrate for protein kinase C. Proc. Natl. Acad. Sci. USA **86:**4012–4016.
28. **Tomkinson, B., E. Robertson, R. Yalamanchili, R. Longnecker, and E. Kieff.** 1993. Epstein-Barr virus recombinants from overlapping cosmid fragments. J. Virol. **67:**7298–7306.
29. **Wang, D., D. Liebowitz, F. Wang, C. Gregory, A. Rickinson, R. Larson, T. Springer, and E. Kieff.** 1988. Epstein-Barr virus latent infection membrane protein alters the human B-lymphocyte phenotype: deletion of the amino terminus abolishes activity. J. Virol. **62:**4173–4184.
30. **Wang, F., C. Gregory, C. Sample, M. Rowe, D. Liebowitz, R. Murray, A. Rickinson, and E. Kieff.** 1990. Epstein-Barr virus latent membrane protein (LMP1) and nuclear proteins 2 and 3C are effectors of phenotypic changes in B lymphocytes: EBNA-2 and LMP1 cooperatively induce CD23. J. Virol. **64:**2309–2318.
31. **Wang, F., C. D. Gregory, M. Rowe, A. B. Rickinson, D. Wand, M. Birkenbach, H. Kikutani, T. Kishimoto, and E. Kieff.** 1987. Epstein-Barr virus nuclear antigen 2 specifically induces expression of the B-cell activation antigen CD23. Proc. Natl. Acad. Sci. USA **84:**3452–3456.
32. **Wang, F., S.-F. Tsang, M. G. Kurilla, J. I. Cohen, and E. Kieff.** 1990. Epstein-Barr virus nuclear antigen 2 transactivates latent membrane protein LMP1. J. Virol. **64:**3407–3416.
33. **Yamashiro-Matsumura, S., and F. Matsumura.** 1985. Purification and characterization of an F-actin-bundling 55-kilodalton protein from HeLa cells. J. Biol. Chem. **260:**5087–5097.
34. **Yamashiro-Matsumura, S., and F. Matsumura.** 1986. Intracellular localization of the 55-kD actin-bundling protein in cultured cells: spatial relationships with actin, alpha-actinin, tropomyosin, and fimbrin. J. Cell Biol. **103:**631–640.
35. **Zuber, M. X., D. W. Goodman, L. R. Karns, and M. C. Fishman.** 1989. The neuronal growth-associated protein GAP-43 induces filopodia in non-neuronal cells. Science **244:**1193–1195.